0026-895X/07/7204-1024–1032
MOLECULAR PHARMACOLOGY
U.S. Government work not protected by U.S. copyright
Mol Pharmacol 72:1024–1032, 2007

Vol. 72, No. 4
36939/3256184
Printed in U.S.A.

The Endocannabinoid Anandamide Inhibits the Function of $\alpha4\beta2$ Nicotinic Acetylcholine Receptors[S]

Charles E. Spivak, Carl R. Lupica, and Murat Oz

United States Department of Health and Human Services, National Institutes of Health, National Institute on Drug Abuse, Intramural Research Program, Cellular Neurobiology Branch, Electrophysiology Research Unit, Baltimore, Maryland

Received April 11, 2007; accepted July 12, 2007

ABSTRACT

The effects of the endocannabinoid anandamide (arachidonylethanolamide, AEA) on the function of $\alpha4\beta2$ nicotinic acetylcholine receptors (nAChR) stably expressed in SH-EP1 cells were investigated using the whole-cell patch-clamp technique. In the concentration range of 200 nM to 2 μM, AEA significantly reduced the maximal amplitudes and increased the desensitization of acetylcholine (ACh)-induced currents. The effects of AEA could be neither replicated by the exogenous cannabinoid Δ^9-tetrahydrocannabinol (1 μM) nor reversed by the selective CB1 receptor antagonist 5-(4-chlorophenyl)-1-(2,4-dichlorophenyl)-4-methyl-*N*-(piperidin-1-yl)-1*H*-pyrazole-3-carboxamide (SR-141716A) (1 μM). The actions of AEA were apparent when applied extracellularly but not during intracellular dialysis. Furthermore, the effects of AEA ACh currents were not altered by the calcium chelator 1,2-bis(2-aminophenoxy)ethane-*N,N,N′,N′*-tetraacetic acid. The onset and washout of the AEA effects required several minutes (10–30 min), but the latter was significantly decreased in the presence of lipid-free bovine serum albumin (BSA). Moreover, BSA alone increased peak ACh current amplitudes and diminished desensitization rates in naive cells, suggesting a tonic modulation of $\alpha4\beta2$ nAChR function by an endogenous AEA-like lipid. Further analysis of AEA effects on $\alpha4\beta2$ nAChR-mediated currents, using a two-stage desensitization model, indicated that the first forward rate constant leading to desensitization, k_1, increased nearly 30-fold as a linear function of the AEA concentration. In contrast, the observation that the other three rate constants were unaltered by AEA suggested that AEA raised the energy of the activated state. These results indicate that AEA directly inhibits the function of $\alpha4\beta2$ nAChRs in a CB1 receptor-independent manner.

Arachidonylethanolamide is an endogenously produced fatty-acid ethanolamide that activates cannabinoid receptors to produce cellular and pharmacological effects similar to Δ^9-THC, the psychoactive component of marijuana (Howlett et al., 2002; Pacher et al., 2006). However, several reports indicate that AEA can produce effects that are not mediated by the activation of the cloned CB1 or CB2 receptors. For example, it has been demonstrated that AEA inhibits the functions of voltage-dependent Ca^{2+} channels (Oz et al., 2000; Chemin et al., 2001), Na^+ channels (Nicholson et al., 2003), various types of K^+ channels (Poling et al., 1996; Oliver, 2004), 5-hydroxytryptamine type 3 receptor function (Barann et al., 2002; Oz et al., 2002), and nicotinic ACh receptors (Oz et al., 2003) in a cannabinoid receptor-independent manner (Oz, 2006). These findings can suggest that additional molecular targets for AEA exist in the CNS.

The nAChR-containing $\alpha4\beta2$ subunit, the predominant subtype in the CNS, has been linked to the positive-reinforcing and cognitive effects of nicotine (Tapper et al., 2004; Brody et al., 2006), and its high affinity for nicotine has led to the proposal that it is a primary target for nicotine's actions in the CNS (Laviolette and van der Kooy, 2004). In support of this view, recent studies with mutant mice demonstrated that the $\alpha4\beta2$ nAChR was necessary to observe tolerance and sensitization to nicotine in vivo (Tapper et al., 2004). Biochemical, electrophysiological, behavioral, and clinical evidence support the existence of functional interactions between nicotinic receptors and cannabinoids, including AEA (Castañé et al., 2005; Viveros et al., 2006). In addition, we have shown that the endogenous cannabinoid AEA inhibits ion currents mediated by the activation of nACh α_7 receptors expressed in *Xenopus laevis* oocytes (Oz et al., 2003).

To date, the functional interaction between $\alpha4\beta2$ nAChR

This study was supported by funds from the Intramural Research Program of the National Institute on Drug Abuse, U.S. Department of Health and Human Services.

Article, publication date, and citation information can be found at http://molpharm.aspetjournals.org.

doi:10.1124/mol.107.036939.

[S] The online version of this article (available at http://molpharm.aspetjournals.org) contains supplemental material.

ABBREVIATIONS: Δ^9-THC, Δ^9-tetrahydrocannabinol; ACh, acetylcholine; AEA, arachidonylethanolamide, anandamide, *N*-(2-hydroxyethyl)-5,8,11,14-eicosatetraenamide (all-*Z*)-; BAPTA, 1,2-bis(2-aminophenoxy)ethane-*N,N,N′,N′*-tetraacetic acid; BSA, bovine serum albumin; CNS, central nervous system; CB1, cannabinoid type 1 receptor; nAChR, nicotinic acetylcholine receptor; SR-141716A, 5-(4-chlorophenyl)-1-(2,4-dichlorophenyl)-4-methyl-N-(piperidin-1-yl)-1H-pyrazole-3-carboxamide; URB 597, cyclohexyl carbamic acid 3′-carbamoylbiphenyl-3-yl ester.

and cannabinoid receptor ligands such as AEA and Δ^9-THC has not been investigated. In the present study, we examine the effects of these cannabinoids on the function of $\alpha4\beta2$ nAChR receptors stably transfected in the SH-EP1 cell line.

Materials and Methods

Cell Culture. The SH-EP1 cells stably expressing the human $\alpha4\beta2$ nAChR, a gift from Dr. R Lukas (Barrow Neurological Institute, Phoenix, AZ), are described elsewhere (Pacheco et al., 2001). They were grown on 35-mm dishes in Dulbecco's modified Eagle's medium (Invitrogen, Carlsbad, CA) supplemented with 10% heat-inactivated horse serum, 5% fetal bovine serum, 1 mM sodium pyruvate, 100 U/ml penicillin G, 100 μg/ml streptomycin, 0.25 μg/ml amphotericin B, 0.4 mg/ml hygromycin B, and 0.25 mg/ml Zeocin (all from Invitrogen). The cells were maintained at 37°C in an atmosphere of 5% CO_2 saturated with H_2O.

Electrophysiological Recording. The cells were recorded at ambient temperature while superfused at 2.0 ml/min with Dulbecco's phosphate-buffered saline augmented with sucrose to match the osmolarity (340 mOsM) of the growth medium. The composition was 136.9 mM NaCl, 2.68 mM KCl, 0.49 mM $MgCl_2$, 0.9 mM $CaCl_2$, 1.47 mM KH_2PO_4, 8.1 mM Na_2HPO_4, 5.55 mM glucose, and 45.0 mM sucrose, pH 7.40. The intracellular solution contained in the patch pipettes was modified to minimize ACh current rundown (Wu et al., 2004) and consisted of 110 mM Tris phosphate dibasic, 28 mM Tris base, 2 mM $MgCl_2$, 0.1 mM $CaCl_2$; 11 mM EGTA, and 1.8 mM $Mg_3(ATP)_2$ brought to pH 7.30 with H_3PO_4. Because this pipette medium has approximately 40% of the specific conductance of a corresponding KCl solution, open pipettes had resistances of 4 to 8 MΩ despite having tip diameters of approximately 1.5 μm. Conventional whole-cell recording conditions were established after first achieving a 1 to 5 GΩ cell-attached seal. The cells were voltage-clamped at −60 mV using an Alembic VE-2 whole-cell amplifier (Alembic Instruments, Montreal, QC, Canada). Series resistance, measured using a 10-mV step before each test, was 100% compensated. Drugs were locally superfused using a modified U-tube (Murase et al., 1989) positioned 35 μm above and 190 μm lateral to the base of the patch-clamped cell. Local superfusion with 150 mM choline chloride in this configuration demonstrated a change in junction potential at an open-tipped pipette with 10 to 90% rise times of 2 to 3 ms. This time sets the lower limit of cellular rise times to ACh application. Acetylcholine was applied to voltage-clamped cells for 4.9 s at 30 μM unless noted otherwise. The currents, recorded using pClamp 7.0 software (Molecular Devices, Sunnyvale, CA), were filtered (low-pass) to 200 Hz and sampled at 1 kHz. The cells generally had ~30 pF capacitance and 60 to 150 MΩ membrane resistance. Data means ± S.E.M. were compiled from three to six cells.

Acetylcholine was used as the agonist to probe receptor function. We preferred it over other agonists mostly because of its low hydrophobicity, making it easy to wash out, and because, unlike nicotine, it has limited ability to desensitize the $\alpha4\beta2$ nAChRs (Paradiso and Steinbach, 2003). Acetylcholine (Sigma, St. Louis, MO) was diluted each day from a 10 mM stock that was prepared weekly. AEA (Tocris Bioscience, Ellisville, MO) was diluted daily from a stock solution prepared in ethanol (14.4 mM) stored at −20°C and dispensed directly into the superfusion solution. SR-141716A and Δ^9-THC were obtained from the National Institute on Drug Abuse Drug Supply System (Bethesda, MD).

Data Analysis. Average values were calculated as mean ± S.E.M. Statistical significance was evaluated using Student's t test. Concentration-response parameters were obtained by fitting the data to the logistic equation $y = E_{max}/(1 + [EC_{50}/x]^{n_H})$, where x and y are concentration and response, respectively, E_{max} is the maximal response, EC_{50} is the half-maximal concentration, and n_H is the slope factor (apparent Hill coefficient). For data analysis and calculations of concentration-response curve data, we used the computer program MLAB (Civilized Software, Bethesda, MD).

The kinetic analyses of the current decays were performed using the modeling program MLAB. A more intuitive explanation is given in the supplementary materials. The kinetic analysis incorporated only the decay phases of the responses because the kinetics of the rising phases were limited by various parameters including the cell size, the unstirred layer (Spivak et al., 2006), and the perfusion rate (see supplementary materials). The decay phase was modeled as a two-stage sequential desensitization process, described in Scheme 1, where AR* represents the activated (open channel) state, AR′, the first desensitized state, and AR″, the second desensitized state. It was assumed that at the peak of the response, AR′ = AR″ = 0. The parameters AR* (initial), k_1, k_{-1}, k_2, and k_{-2} were fitted simultaneously by nonlinear regression analysis to each decay.

Results

Acetylcholine Concentration Response. ACh-induced inward currents were elicited using various concentrations of the agonist at a fixed treatment time of 4.9 s and were delivered in random order to voltage-clamped cells (Fig. 1). These currents were mediated by the nAChR, as these cells are devoid of muscarinic receptors (Lambert et al., 1989). ACh application evoked an inward current whose amplitude was dependent on its concentration. A maximal activation of this current was seen at approximately 100 μM ACh, and the EC_{50} was 40 ± 5 μM. Rise times (10–90%) for the ACh-evoked currents were <100 ms, and typically were approximately 50 ms, which was approximately 20 times greater

$$AR^* \underset{k_{-1}}{\overset{k_1}{\rightleftharpoons}} AR' \underset{k_{-2}}{\overset{k_2}{\rightleftharpoons}} AR''$$

Scheme 1. Kinetic scheme showing the agonist-bound and activated (conducting) nAChR, denoted AR*, sequentially converting to desensitized states AR′ and AR″ by the first order forward and backward rate constants k_1, k_{-1}, k_2, and k_{-2}, respectively.

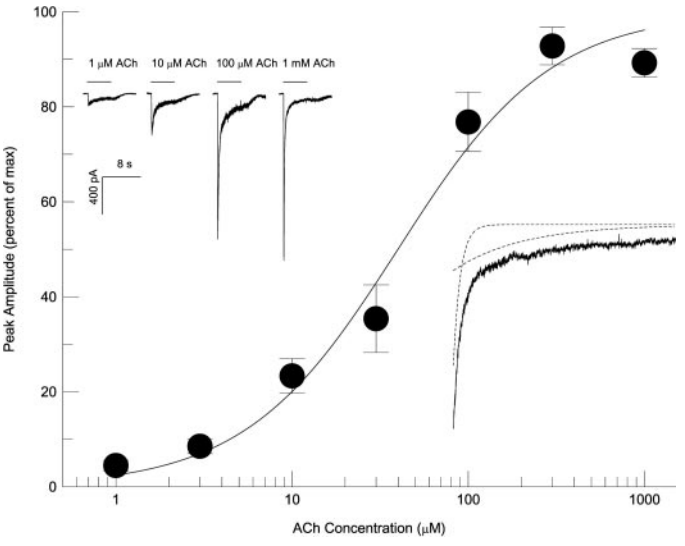

Fig. 1. Peak amplitudes, normalized to the maximum observed for each cell, are shown plotted as a function of the ACh concentration at the SH-EP1 cells stably expressing the $\alpha4\beta2$ nAChR. The cells were voltage-clamped to −60 mV using the whole-cell technique. Means ± S.E.M. are shown. The left inset shows typical current traces in a single cell at various concentration of ACh, and the right inset shows the decomposition of the response to 100 μM ACh into its two exponential components.

than the time required for solution change (see *Materials and Methods*). The responses usually decayed as double-exponential functions of time, reflecting two phases of desensitization (see *Materials and Methods*). At low ACh concentrations, double-exponential decays became difficult or impossible to discern from single exponentials because the signal was smaller and because k_1 approached k_2 (Fig. 2, A and C). As a result, parameters for the second stage of desensitization were more prone to error or were impossible to obtain (such as the k_2 and k_{-2} values for 1 μM ACh in Fig. 2). Figure 2 depicts the relationships between the fitted rate constants to the ACh concentration. The rate constant k_1 increased approximately 16-fold as a function of the ACh concentration (1–1000 μM; Fig. 2A) and was directly proportional to the activated state AR* (Fig. 2B), as required by the desensitization scheme. In contrast, k_2 showed only a slight tendency to increase with the ACh concentration (Fig. 2C) with no correlation to the activated state (Fig. 2D). The backward rate constants, k_{-1} and k_{-2}, showed no change with ACh concentration (Fig. 2, E and F). These relationships are consistent with the desensitization scheme above.

Effects of AEA on $\alpha 4\beta 2$ nAChR Kinetics. Figure 3A illustrates the three features of the AEA effect on ACh responses: 1) a decrease in peak amplitude; (2) an increase in the decay rate of the more rapid phase of the response; and 3) that these effects increase gradually over tens of minutes. The decreases of peak amplitude are summarized in Fig. 3B, which shows that the progressive decrease in normalized peak amplitudes required at least 20 min of exposure to AEA and increased with the AEA concentration. Exponential time constants are 12.2, 12.2, 6.1, and 4.4 min for AEA concentrations of 0.2, 0.5, 1, and 2 μM, respectively. From inspection of Fig. 3B, one obtains an estimate of IC_{50} (at 20 min) of approximately 300 nM. AEA concentrations greater than 2 μM were not systematically tested because the ACh currents were completely inhibited.

The decays of the ACh-induced currents in the presence of AEA were fitted to the desensitization scheme given above to derive the four rate constants. Figure 3C shows that the values of the first forward rate constant for desensitization k_1, determined for AEA concentrations up to 2 μM, increased as exponential functions of time, and their asymptotic max-

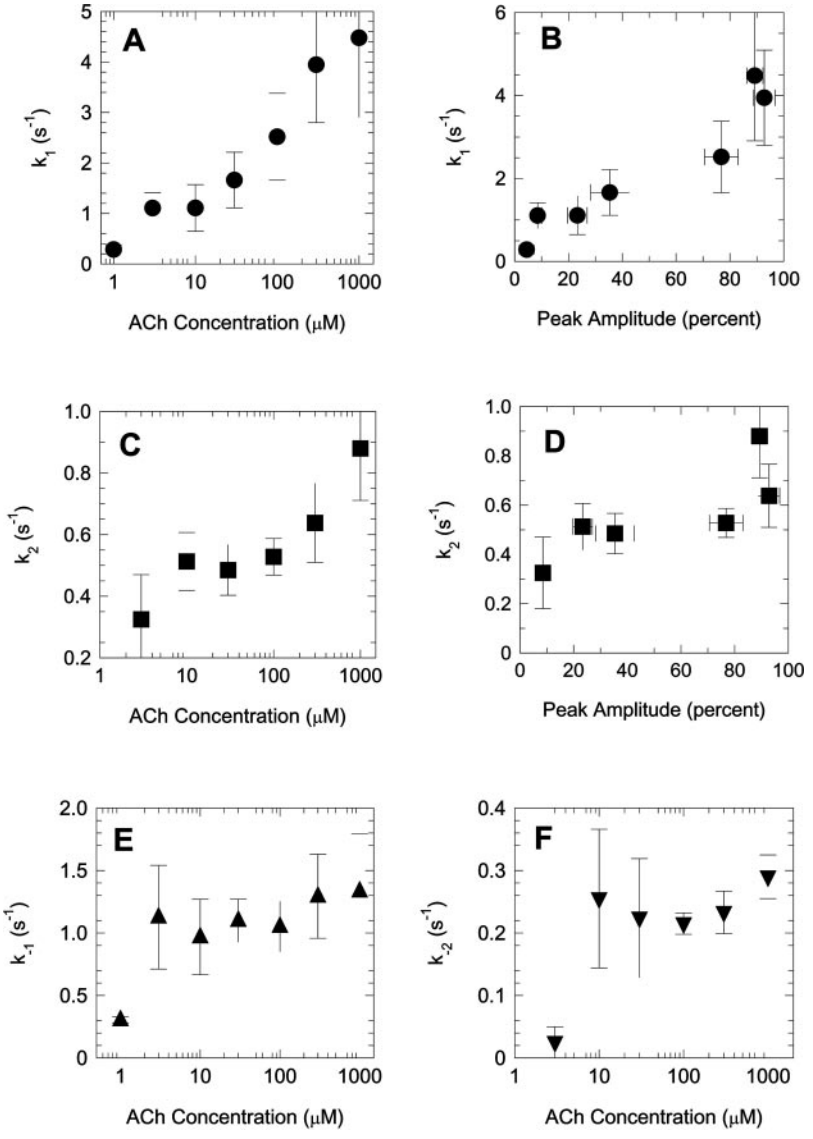

Fig. 2. Kinetics of desensitization as a function of the ACh concentration. The decays of the responses to ACh were analyzed according to the model of two sequential states denoted by Scheme 1 to yield the four rate constants. A, C, E, and F plot the four rate constants as functions of the ACh concentration. B and D are scatter plots of the peak amplitudes versus forward rate constants $k_1$and k_2, respectively. Symbols represent means ± S.E.M.

ima increased as linear functions of the AEA concentration (Fig. 3D) with no sign of saturation. In contrast, the estimates of all of the remaining rate constants were independent of time and insensitive to AEA (Fig. 3, E–G).

We next investigated whether cannabinoid receptors were involved in the inhibitory effects of AEA on $\alpha 4\beta 2$ nAChR function or whether there were also direct effects of other cannabinoid ligands on this nAChR. The primary psychoac-

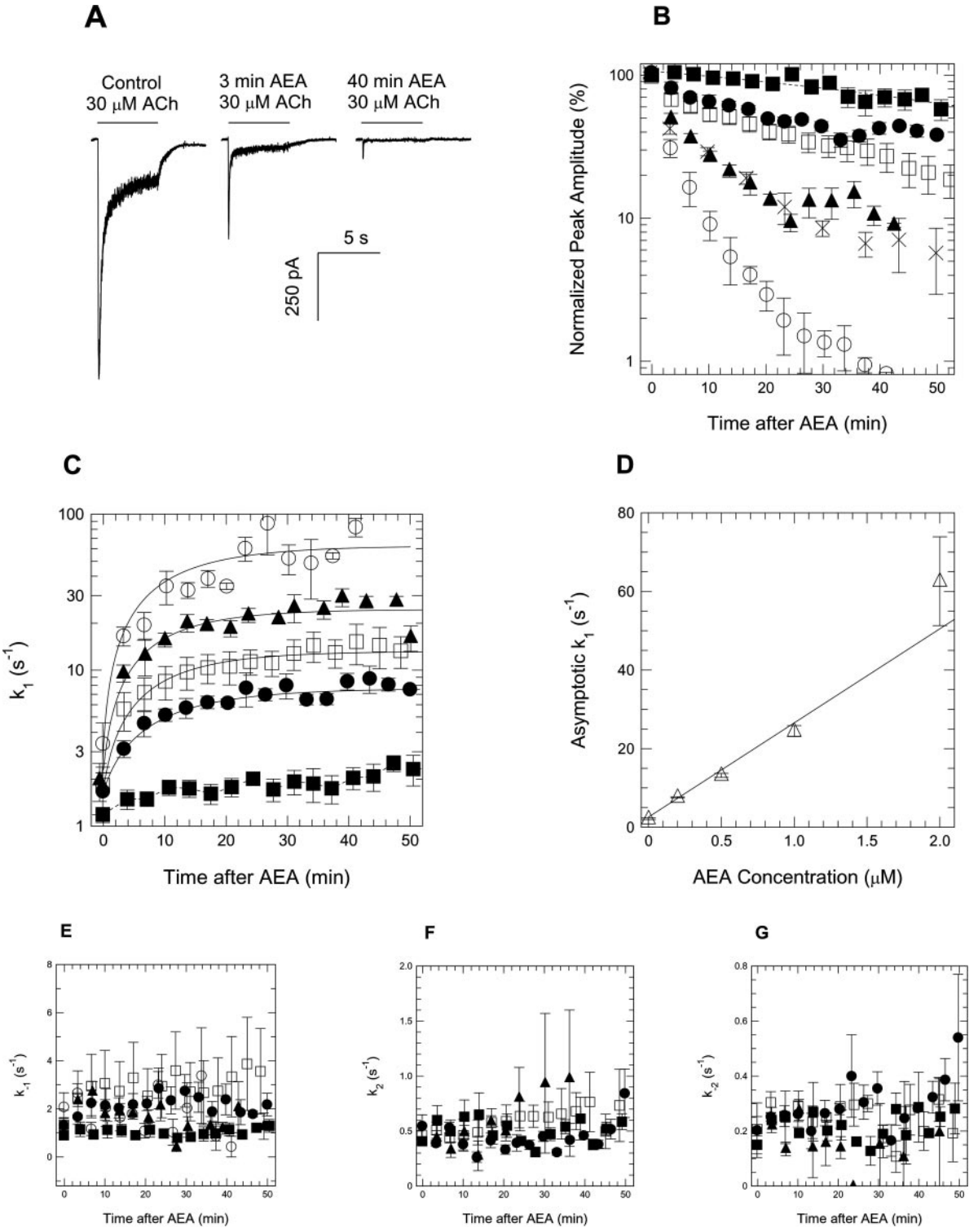

Fig. 3. The effects of AEA on responses to 30 μM ACh. A, representative responses of a cell under control condition followed by continuous superfusion of 1 μM AEA for 3 and 40 min. B, normalized peak amplitudes are plotted as a function of time and concentration of AEA. Filled squares (■) represent the control condition; filled circles (●), 200 nM AEA; open squares (□), 500 nM AEA; filled triangles (▲) and X symbols (at 6-min intervals), 1 μM AEA; and open circles (○), 2 μM AEA. The desensitization rate constants are shown plotted as a function of time in C, E, F, and G. Asymptotes of the k_1 values, taken from C, are plotted as a function of the AEA concentration in D with uncertainties obtained from fitting the curves in C to an exponential function.

tive constituent of cannabis, Δ^9-THC (1 μM), did not alter the amplitudes or the kinetics of the current elicited by ACh (Fig. 4). In addition, the cannabinoid receptor antagonist SR-141716A (rimonabant), which had no effect by itself on ACh responses ($n = 3$), did not significantly alter the effects of AEA on the $\alpha4\beta2$ nAChR (Fig. 5, A and C–E). However, SR-141716A did seem to reverse slightly the effect of AEA on rate constant k_1 (Fig. 5B).

The site of the AEA action was further tested by including the endocannabinoid (1 μM) in the pipette solution. To prevent possible hydrolysis of AEA to arachidonic acid by fatty-acid amide hydrolase, 1 μM URB 597, the specific and potent fatty-acid amide hydrolase inhibitor (Kathuria et al., 2003) was included in the patch pipette. Application of ACh at 3-min intervals for up to 40 min showed a rundown of peak amplitudes to 80 ± 11% ($n = 6$), which was indistinguishable from the control value of 88 ± 5% ($n = 4$; $P > 0.5$). In addition, the value of the first forward rate constant for desensitization, k_1, increased slightly from 1.52 ± 0.34/s to 1.96 ± 0.61/s at 30 min ($n = 6$), values that are in complete agreement with controls ($P > 0.4$) and in striking contrast to the effects of 1 μM AEA applied extracellularly (Fig. 3C). These results require more thorough study, however, because hydrophobic compounds may not be efficiently delivered by means of a patch pipette (Akk et al., 2005).

In earlier studies, AEA has been shown to increase intracellular Ca^{2+} levels (Oz, 2006). Furthermore, the $\alpha4\beta2$ nAChR is permeable to Ca^{2+} (Fucile, 2004), and various second-messenger cascades activated by increased levels of intracellular Ca^{2+} could modulate the function of these receptors and mimic the actions of AEA. For this reason, we tested the effect of the high-affinity, fast-acting calcium chelator BAPTA on AEA inhibition of the $\alpha4\beta2$ nAChR. However, inclusion of BAPTA (11 mM) in the pipette solution did not alter the effects of extracellular AEA on the peak amplitudes and desensitization rates of the $\alpha4\beta2$ nAChR-mediated currents. Thus, after 30 min of 1 μM AEA treatment, peak amplitudes for BAPTA versus control were 10.8 ± 4.1 ($n = 3$) and 13.0 ± 3.7% ($n = 3$) of the initial values, respectively ($P > 0.3$). The corresponding values of k_1 were 19.0 ± 4.3/s ($n = 3$) and 25.3 ± 5.2/s ($n = 4$), respectively ($P > 0.4$). To avoid the possibility of any local increase in unbuffered Ca^{2+} concentration, we replaced calcium with equimolar barium in the extracellular medium and tested the effects of 0.5 μM AEA on 30 μM ACh responses. On comparing the results with those obtained in calcium-containing medium, we found no change in peak amplitudes and rate constants k_{-1}, k_2, and k_{-2} (4 or 5 cells, monitored for 40 min). The rate constant k_1, however, was 61 ± 3% of the corresponding value in calcium-containing medium for all time points, including those before the application of AEA. Because of the constant percentage of decrease of k_1 on the cells even before AEA treatment, we believe that the barium-containing medium, rather than antagonizing AEA directly, lowered the free energy of the activated state and that the barium and AEA effects were independent and additive.

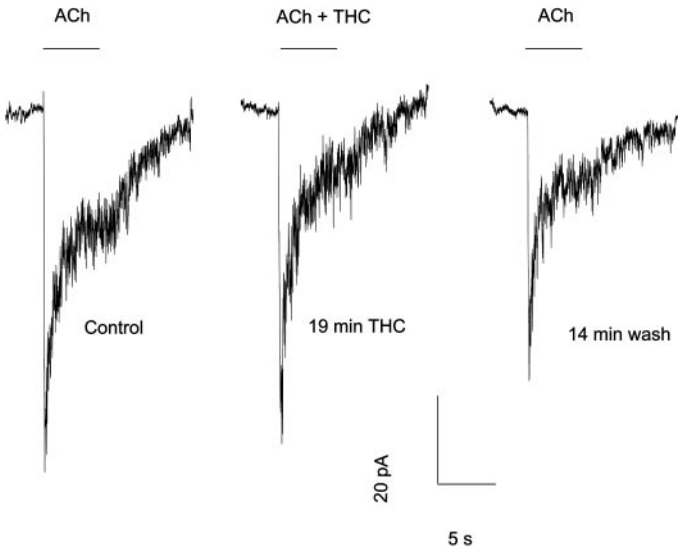

Fig. 4. Representative traces for responses of a cell to 30 μM ACh under control condition after 14 min of continuous superfusion of 1 μM Δ^9-THC and after the washout of the Δ^9-THC.

An open-channel blockade, by definition, requires the opening of the channel by the binding of agonist to the receptor. Thus, in the absence of an agonist, pretreatment with a blocker should not cause inhibition, and the degree of blockade should be related to the frequency of channel activation. Therefore, the extent of AEA inhibition of the $\alpha4\beta2$ nAChR-mediated response was compared in cells exposed to ACh at 6-min intervals with those exposed at 3-min intervals. However, increasing the ACh test interval to 6 min during AEA (1 μM) application gave responses indistinguishable from those tested at the 3-min interval, indicating that the block by AEA was not use-dependent (Fig. 3B).

If the slow onset of the AEA effects was a consequence of its partitioning into the lipid membrane, then the time course of reversal of the AEA effect should be similar to onset during simple washout but greatly enhanced if a lipid scavenger is included in the extracellular solution. The offset kinetics were first tested under normal conditions (Fig. 6, A and B). Because our objective was to characterize the reversal of the AEA treatment by monitoring this phase as long as possible, we applied the endocannabinoid for only 3 min before beginning the wash phase. This application period is seen in Fig. 6, A and B, as the gap between the last control test and the first test after beginning the wash period denoted by the pair of dotted vertical lines. The peak ACh-induced current amplitudes were reduced to 60% of control by this application of AEA and intersected the control rundown curve at approximately 50 min after the start of the wash (Fig. 6A, broken line, taken from Fig. 3B). The recovery of the k_1 values were clearer, approaching the control value during the wash phase as an exponential function of time with a time constant of 30 ± 4 min (Fig. 6B). In the next series of experiments, we recorded control responses to ACh in BSA-free medium. The cells were then treated with 1 μM AEA for 10 min followed by a wash with 1 mg/ml of lipid-free BSA (Poling et al., 1996). Figure 6, C and D, reveal that the recovery of peak amplitudes and k_1 were complete by 9 min, an order of magnitude faster than recovery without BSA (the time constants were 2.2 and 1.7 min, respectively). In addition, the amplitudes of the ACh-evoked currents during BSA treatment seemed to be larger than those observed during the control baseline period, observed before AEA application (Fig. 6C). We speculated that this might result from the tonic inhibition of the $\alpha4\beta2$ nAChR by an endogenous lipid molecule that was sensitive to BSA. To test this hypothesis, we examined the

effects of BSA on ACh-evoked currents in the absence of AEA application (Fig. 7). Treatment with BSA alone (14 min) caused significant effects on peak amplitudes of the α4β2 nAChR currents and the rate constant k_1 that were opposite to those caused by AEA. Furthermore, the effects of BSA were reversible by a brief washing with control saline. BSA had no effects on the other rate constants.

Discussion

The present results indicate that the endocannabinoid AEA inhibited the function of the α4β2 nAChR in a cannabinoid receptor-independent manner. Furthermore, this effect was relatively selective for this cannabinoid receptor agonist because the phytochemical agonist Δ^9-THC was ineffective in modulating nAChR-mediated ion currents, and the cannabinoid antagonist SR-141716A did not affect the AEA inhibition of α4β2 nAChR function. These results therefore indicate that AEA acts directly at the α4β2 nAChR independently of cannabinoid receptors to modulate the strength of nicotinic signaling. In agreement with these results, AEA has also been found to modulate the functions of other voltage-gated (Poling et al., 1996; Oz et al., 2000; Oliver et al., 2004; Fisyunov et al., 2006) and ligand-gated (Barann et al., 2002; Oz et al., 2002, 2003, 2004b) ion channels and other integral membrane proteins at a similar concentration range and in a cannabinoid receptor-independent manner (Oz, 2006).

The α4β2 nAChR is highly permeable to Ca^{2+} (Fucile, 2004), and the nAChR-induced increases in intracellular Ca^{2+} levels can activate various second messengers that modulate the function of the receptors in a feedback fashion (Fenster et al., 1999). However, in the present work, the inclusion of BAPTA in the pipette solution and the replacement of extracellular Ca^{2+} with Ba^{2+} did not alter the AEA inhibition of the α4β2 nAChR, suggesting that the changes in the intracellular Ca^{2+} levels were not involved in AEA actions on these receptors. In other studies, the ability of AEA to inhibit the function of ion channels (Oz, 2006) has been ascribed to an action at an intracellular binding site. To test this hypothesis, we dialyzed the cell with AEA in the pipette, and ACh produced currents with amplitudes and decay kinetics that were indistinguishable from controls, suggesting that the site of AEA action was extracellular. However, given the rapid traverse of fatty acids across phospholipid mem-

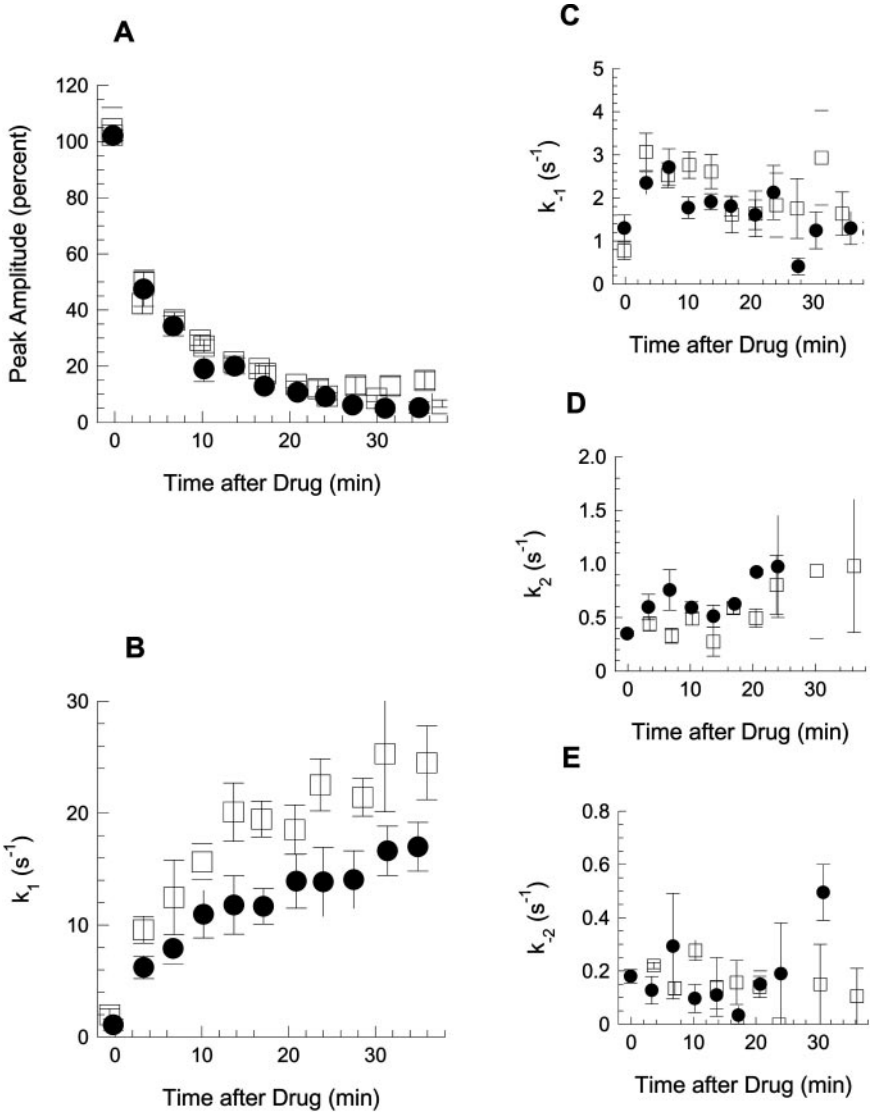

Fig. 5. Effects of 1 μM SR-141716A on peak amplitudes and desensitization rate constants on responses to 30 μM ACh in the continuous presence of 1 μM AEA. Squares represent control values (with AEA but in the absence of SR-141716A), and circles represent values obtained in the presence of SR-141716A. Symbols represent means ± S.E.M.

branes (Kamp and Hamilton, 1993) and the caution required in interpreting intracellular application of hydrophobic substances (Akk et al., 2005), we view the site of AEA action as inconclusive.

In agreement with earlier findings (Paradiso and Steinbach, 2003; Wu et al., 2004), $\alpha4\beta2$ nAChR currents in voltage-clamped SH-EP1 cells decayed with double-exponential kinetics, which can be analyzed as two mechanistic states of desensitization (Scheme 1). Through a simplification of comprehensive schemes (Quick and Lester, 2002; Paradiso and Steinbach, 2003), Scheme 1 was useful because it accounted for the data by ascribing a mechanism to the decays in the ACh currents, both alone and in the presence of AEA. Thus, the rate constant k_1, which leads from the activated to the first desensitized state, was found to be a function of the ACh concentration (Fig. 1A) and was directly proportional to the activated state (AChR* of Scheme 1) of the nAChR (Fig. 1B), whereas the other rate constants were independent of these variables (Fig. 1, C–F). Therefore, this model parsimoniously described our data while providing mechanistic insight into the desensitization of the $\alpha4\beta2$ nAChR by AEA. The most striking effect of AEA in this model was the linear increase in the value of k_1 with increasing AEA concentrations, such that at 2 μM AEA, it was 27-fold higher than the control value. The other rate constants remained unchanged by AEA. This selectivity can be understood in terms of energy states of the $\alpha4\beta2$ nAChR. If the activation energy barrier between the activated (AChR*) and the first desensitized state (AChR′; Scheme 1) was lowered by AEA (Fig. 8, dotted line), then both k_1 and k_{-1} would have increased. However, if AEA increased the energy of the activated state AR* (Fig. 8, broken curve), then only k_1 would increase, as observed. This explanation implies that AEA will cause a faster closure rate of the open ion channel and hence a reduction in peak amplitudes due to a lower open probability of the ion channel. These predictions are testable by single-channel recording experiments that are currently in progress.

Open-channel blockade is the most widely used model to describe the block of ligand-gated ion channels. However, this model is inappropriate to describe the present data for the following reasons. First, under conditions of low free concentrations of a blocking ligand, such as AEA, no occlusion should occur. Therefore, in the present data, the scavenging of free AEA by BSA should be especially effective in preventing open-channel blockade, but 3 min after BSA treatment, the decay (expressed as $k_{1)}$ was still accelerated (Fig. 6D). Second, there was an absence of use-dependent blockade (Fig. 3B), and AEA had almost no effect when coadministered with ACh without preincubation (data not shown). Open-channel blockade could occur in the absence of AEA in free solution if AEA first dissolved into the lipid membrane and diffused into a nonannular lipid space to block the ion channel. Scheme 1, validated by the ACh con-

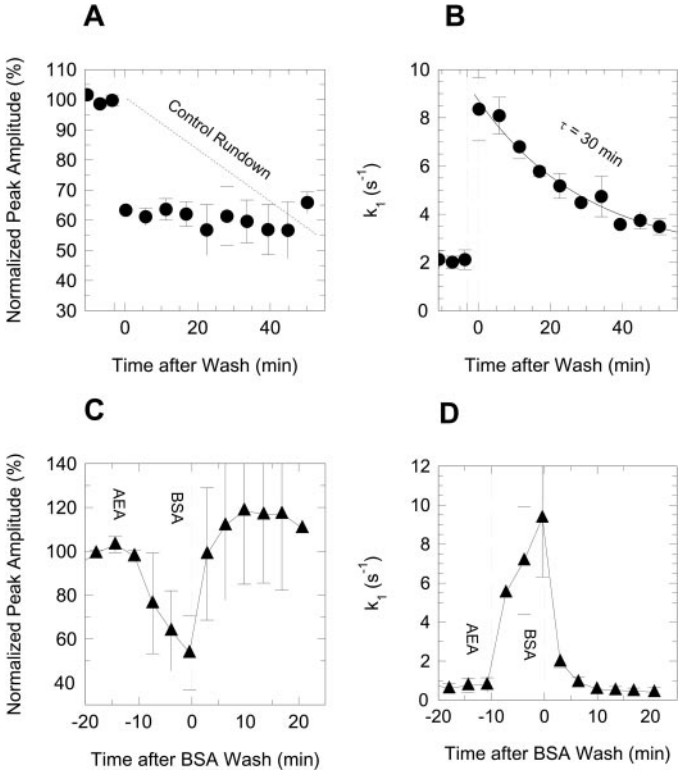

Fig. 6. Lipid-free BSA accelerated the recovery from AEA treatment. The effects on peak amplitudes and desensitization rate constant k_1 are shown in left and right columns, respectively. A and B show the control condition, in which cells were treated with AEA (1 μM) for 3 min (first vertical dotted line) immediately before the wash denoted as time = 0 (second dotted line). The broken line in A represents the rundown of peak amplitudes under AEA-free conditions taken from the broken line in Fig. 3B. C and D show similar experiments in which the cells were treated with AEA for 10 min followed by wash with medium containing BSA at 1 mg/ml.

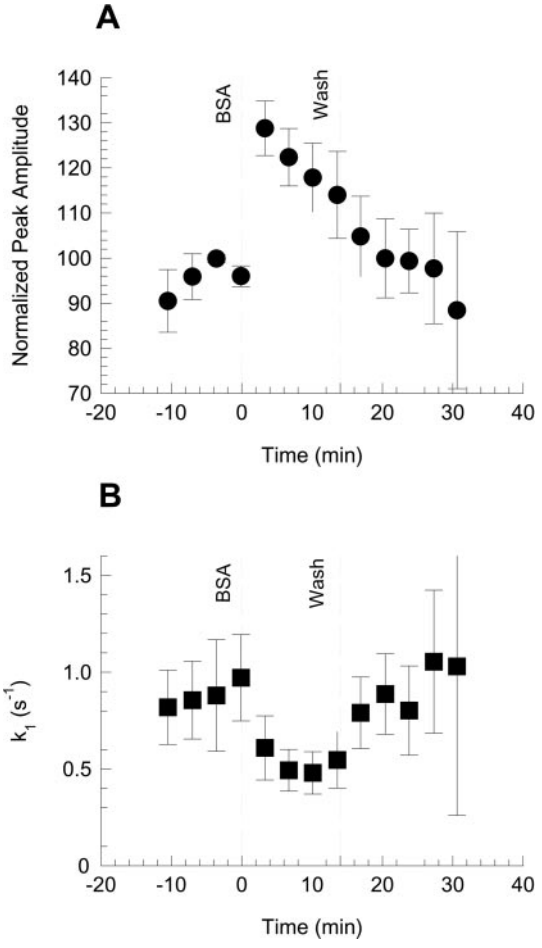

Fig. 7. Effects of BSA (1 mg/ml) on naive cells. The effects of BSA on peak amplitudes (A) and desensitization rate constant k_1 (B) are shown.

centration-response curves, would then be enlarged by adding a second pathway from the activated to the blocked state. Because this model predicted alterations in all four parameters that we did not observe, we therefore conclude that Scheme 1 remains the most parsimonious and useful model for the data.

The striking decrease in the peak amplitudes seen in the presence of AEA could be a consequence of the increase in the rate of desensitization (k_1), as described in our model. It is important to understand that, whereas the fastest perfusion-limited rise time that can be observed in our system is the 2- to 3-ms rise time of the junction potential occurring with a solution change, the rise time for the ACh currents was ~40 ms. This discrepancy probably reflects the time required for ACh to diffuse through the unstirred layer of extracellular solution that surrounds cultured cells under the present conditions. A similar kinetic slowing of the effects of the opioid antagonist naloxone (Spivak et al., 2006) and AEA (Bojesen and Hansen, 2006) by the unstirred layer also has been described recently. In the presence of AEA, this may have led to a desensitization gradient across the cell in which nAChRs in regions of the cell membrane that were activated first by ACh desensitized before more distal nAChRs were activated. Simulations (see supplemental information) that convolve this diffusion of ACh through the unstirred layer with $\alpha4\beta2$ nAChR desensitization show that approximately 80% of the decrease in response amplitude can be attributed to this mechanism. A consistent and parsimonious explanation for the remainder of the decrease is to ascribe it to desensitization of the nAChR in the closed state, a process supported by previous work of others and which seems particularly important for the agonist nicotine (Paradiso and Steinbach, 2003)

Another result of the kinetic analysis was that the increase in k_1 showed no sign of approaching saturation over the entire effective range of AEA concentrations (Fig. 3D). This is consistent with our molecular view of the effect of AEA on ion channels. Given an estimated octanol-water partition coefficient of 1.7×10^5 (LogP from ChemDraw; CambridgeSoft, Cambridge, MA), it is likely that AEA will easily partition into the biological membrane, where it can rapidly displace some of the ~40 annular (Ellena et al., 1983) and possibly the nonannular lipids that are in intimate contact with the receptor. Such alterations of the lipid environment, which include hydrophobic mismatch between lipids and proteins, changes in membrane viscosity, changes in the interfacial curvature, altered lateral pressure profile, and shifts in lipid dipole potential and surface potential can alter the functions of transmembrane proteins (Barrantes, 2004; Lundbaek, 2006). Specifically, we propose that AEA has raised the free energy of the activated state AR*.

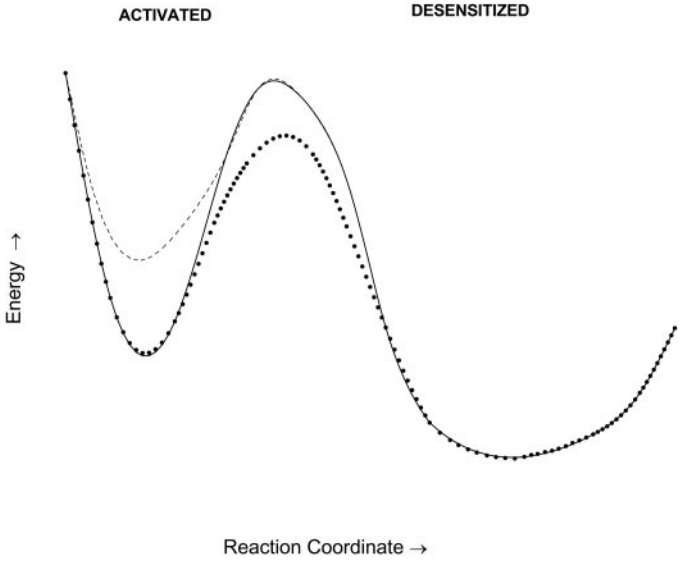

Fig. 8. Hypothetical potential energy versus reaction coordinate plot showing the energies of the activated receptor AR*, the transition state, and the first desensitized state AR′ (see Scheme 1) under the control condition (solid curve) and conditions in which the activation energy is reduced (dotted curve) and in which the energy of the activated state is raised (broken curve). Only the latter alternative would solely increase k_1.

Anandamide belongs to a larger group of signaling lipids consisting of amides of long-chain polyunsaturated fatty acids (Howlett et al., 2002). Earlier studies on nAChRs demonstrated that fatty acids could modulate their function via a direct action (Barrantes, 2004). Thus, it is possible that AEA and fatty acid-based molecules may share common sites of action on various membrane proteins (Oz, 2006). Depending on local concentrations under basal conditions, the modulatory actions of AEA on nAChRs might be tonically present and phasically elevated by neuronal activity that results in the release of this and possibly other endocannabinoids (Freund et al., 2003). Evidence exists for both possibilities in the CNS. For example, the exposure of neurons to long-term ethanol treatment results in an increased accumulation of AEA (Basavarajappa and Hungund, 2002), and long-term ethanol intake increases AEA levels in various brain regions involved in drug abuse (Gonzalez et al., 2004). Thus, alterations in AEA levels in the CNS by abused drugs and/or other pathophysiological conditions may cause changes in tonic activity of nAChRs and/or alter the actions of other abusive substances such as ethanol on nAChR function (Oz et al., 2005). In addition, our study provides further support for the idea that AEA may tonically inhibit $\alpha4\beta2$ nAChRs, because the effects of exogenously applied AEA were reversed by lipid scavenging with BSA (Bojesen and Hansen, 2003), and $\alpha4\beta2$ nAChR function was increased by BSA in naive cells. Also consistent with this proposal is the observation that direct manipulation of the membrane lipid composition causes significant alterations in the activity of nicotinic receptors (Baenziger et al., 2000), suggesting that nAChRs do indeed function under the tonic influence of membrane lipids.

In the central nervous system, $\alpha4\beta2$ nACh receptors are located both pre- and postsynaptically and play an important modulatory role in synaptic transmission (Sher et al., 2004; Dani and Bertrand, 2007). Because AEA acts at the nAChR at physiologically relevant concentrations (Oz, 2006) and given the presence of $\alpha4\beta2$ nACh receptors in these critical locations, it is possible that the activity of the $\alpha4\beta2$ nACh receptor function is regulated by both tonic and phasic AEA in situ. Whereas the $\alpha4\beta2$ nACh receptor represents a novel molecular target for AEA, interactions observed previously between Δ^9-THC and systemic nicotinic pharmacology (Castañé et al., 2005; Viveros et al., 2006) cannot be explained by our findings. Other studies indicate that the function of 5-hydroxytryptamine type 3 receptor and glycine receptors are also modulated by AEA and by Δ^9-THC (Barann et al., 2002; Oz et al., 2002; Hejazi et al., 2006). However, the present results indicate that AEA but not Δ^9-THC inhibits $\alpha4\beta2$

nAChR function. Likewise, differential effects of AEA and Δ^9-THC have been reported on Ca^{2+} channels (Oz et al., 2004b), K^+ channels (Poling et al., 1996), α_7-nAChRs (Oz et al., 2004a), and *N*-methyl-D-aspartate receptors (Hampson et al., 1998), suggesting that AEA and Δ^9-THC do not share a common binding site among various membrane proteins. In conclusion, our results indicate that AEA inhibits the function of $\alpha4\beta2$ nAChRs and suggest that these receptors may represent a novel target for the actions of AEA in the nervous system.

Acknowledgments

We thank Dr. Ronald J. Lukas (Barrow Neurological Institute, Phoenix, AZ) for providing the SH-EP1 cell line stably expressing the $\alpha_4\beta_2$ nAChR. We are indebted to Carol Beglan for expert maintenance of the SH-EP1 cell line.

References

Akk G, Shu HJ, Wang C, Steinbach JH, Zorumski CF, Covey DF, and Mennerick S (2005) Neurosteroid access to the GABAA receptor. *J Neurosci* **25:**11605–11613.
Baenziger JE, Morris ML, Darsaut TE, and Ryan SE (2000) Effect of membrane lipid composition on the conformational equilibria of the nicotinic acetylcholine receptor. *J Biol Chem* **275:**777–784.
Barann M, Molderings G, Bruss M, Bonisch H, Urban BW, and Gothert M (2002) Direct inhibition by cannabinoids of human 5-HT3A receptors: probable involvement of an allosteric modulatory site. *Br J Pharmacol* **137:**589–596.
Barrantes FJ (2004) Structural basis for lipid modulation of nicotinic acetylcholine receptor function. *Brain Res Brain Res Rev* **47:**71–95.
Basavarajappa BS and Hungund BL (2002) Neuromodulatory role of the endocannabinoid signaling system in alcoholism: an overview. *Prostaglandins Leukot Essent Fatty Acids* **66:**287–299.
Bojesen IN and Hansen HS (2003) Binding of anandamide to bovine serum albumin. *J Lipid Res* **44:**1790–1794.
Bojesen IN and Hansen HS (2006) Effect of an unstirred layer on the membrane permeability of anandamide. *J Lipid Res* **47:**561–570.
Brody AL, Mandelkern MA, London ED, Olmstead RE, Farahi J, Scheibal D, Jou J, Allen V, Tiongson E, Chefer SI, et al. (2006) Cigarette smoking saturates brain alpha 4 beta 2 nicotinic acetylcholine receptors. *Arch Gen Psychiatry* **63:**907–915.
Castañé A, Berrendero F, and Maldonado R (2005) The role of the cannabinoid system in nicotine addiction. *Pharmacol Biochem Behav* **81:**381–386.
Chemin J, Monteil A, Perez-Reyes E, Nargeot J, and Lory P (2001) Direct inhibition of T-type calcium channels by the endogenous cannabinoid anandamide. *EMBO J* **20:**7033–7040.
Dani JA and Bertrand D (2007) Nicotinic acetylcholine receptors and nicotinic cholinergic mechanisms of the central nervous system. *Annu Rev Pharmacol Toxicol* **47:**699–6729.
Ellena JF, Blazing MA, and McNamee MG (1983) Lipid-protein interactions in reconstituted membranes containing acetylcholine receptor. *Biochemistry* **22:**5523–5535.
Fenster CP, Beckman ML, Parker JC, Sheffield EB, Whitworth TL, Quick MW, and Lester RA (1999) Regulation of $\alpha4\beta2$ nicotinic receptor desensitization by calcium and protein kinase C. *Mol Pharmacol* **55:**432–443.
Fisyunov A, Tsintsadze V, Min R, Burnashev N, and Lozovaya NA (2006) Cannabinoids modulate the P-type high voltage-activated calcium currents in Purkinje neurons. *J Neurophysiol* **96:**1267–1277.
Freund TF, Katona I, and Piomelli D (2003) Role of endogenous cannabinoids in synaptic signaling. *Physiol Rev* **83:**1017–1066.
Fucile S (2004) Ca^{2+} permeability of nicotinic acetylcholine receptors. *Cell Calcium* **35:**1–8.
Gonzalez S, Valenti M, de Miguel R, Fezza F, Fernandez-Ruiz J, Di Marzo V, and Ramos JA (2004) Changes in endocannabinoid contents in reward-related brain regions of alcohol-exposed rats, and their possible relevance to alcohol relapse. *Br J Pharmacol* **143:**455–464.
Hampson AJ, Bornheim LM, Scanziani M, Yost CS, Gray AT, Hansen BM, Leonoudakis DJ, and Bickler PE (1998) Dual effects of anandamide on NMDA receptor-mediated responses and neurotransmission. *J Neurochem* **70:**671–676.
Hejazi N, Zhou C, Oz M, Sun H, Ye JH, and Zhang L (2006) Δ9-Tetrahydrocannabinol and endogenous cannabinoid anandamide directly potentiate the function of glycine receptors. *Mol Pharmacol* **69:**991–997.
Howlett AC, Barth F, Bonner TI, Cabral G, Casellas P, Devane WA, Felder CC, Herkenham M, Mackie K, Martin BR, et al. (2002) International Union of Pharmacology. XXVII. Classification of cannabinoid receptors. *Pharmacol Rev* **54:**161–202.
Kamp F and Hamilton JA (1993) Movement of fatty acids, fatty acid analogues, and bile acids across phospholipid bilayers. *Biochemistry* **32:**11074–11086.
Kathuria S, Gaetani S, Fegley D, Valino F, Duranti A, Tontini A, Mor M, Tarzia G, La Rana G, Calignano A, et al. (2003) Modulation of anxiety through blockade of anandamide hydrolysis. *Nat Med* **9:**76–81.
Lambert DG, Ghataorre AS, and Nahorski SR (1989) Muscarinic receptor binding characteristics of a human neuroblastoma SK-N-SH and its clones SH-SY5Y and SH-EP1. *Eur J Pharmacol* **165:**71–77.
Laviolette SR and van der Kooy D (2004) The neurobiology of nicotine addiction: bridging the gap from molecules to behaviour. *Nat Rev Neurosci* **5:**55–65.
Lundbaek JA (2006) Regulation of membrane protein function by lipid bilayer elasticity - a single molecule technology to measure the bilayer properties experienced by an embedded protein. *J Phys Condens Matter* **18:**S1305–S1344.
Murase K, Ryu PD, and Randic M (1989) Excitatory and inhibitory amino acids and peptide-induced responses in acutely isolated rat spinal dorsal horn neurons. *Neurosci Lett* **103:**56–63.
Nicholson RA, Liao C, Zheng J, David LS, Coyne L, Errington AC, Singh G, and Lees G (2003) Sodium channel inhibition by anandamide and synthetic cannabimimetics in brain. *Brain Res* **978:**194–204.
Oliver D, Lien CC, Soom M, Baukrowitz T, Jonas P, and Fakler B (2004) Functional conversion between A-type and delayed rectifier K^+ channels by membrane lipids. *Science* **304:**265–270.
Oz M (2006) Receptor-independent actions of cannabinoids on cell membranes: focus on endocannabinoids. *Pharmacol Ther* **111:**114–144.
Oz M, Jackson S, Woods A, Morales M, and Zhang L (2005) Additive effects of endogenous cannabinoid anandamide and ethanol on α7-nicotinic acetylcholine receptor-mediated responses in *Xenopus* oocytes. *J Pharmacol Exp Ther* **313:**1272–1280.
Oz M, Ravindran R, Zhang L, and Morales M (2003) Endogenous cannabinoid, anandamide inhibits neuronal nicotinic acetylcholine receptor-mediated responses in *Xenopus* oocytes. *J Pharmacol Exp Ther* **306:**1003–1010.
Oz M, Ravindran R, Zhang L, Morales M, and Lupica CR (2004a) Direct and differential effects of cannabinoid receptor ligands on α_7-nicotinic receptor-mediated currents in *Xenopus* oocytes. *J Pharmacol Exp Ther* **310:**1152–1160.
Oz M, Tchugunova Y, and Dinc M (2004b) Differential effects of endocannabinoids and synthetic cannabinoids on voltage-dependent calcium fluxes in rabbit T-tubule membranes: comparison with fatty acids. *Eur J Pharmacol* **502:**47–58.
Oz M, Tchugunova YB, and Dunn SM (2000) Endogenous cannabinoid anandamide directly inhibits voltage-dependent Ca^{2+} fluxes in rabbit T-tubule membranes. *Eur J Pharmacol* **404:**13–20.
Oz M, Zhang L, and Morales M (2002) Endogenous cannabinoid, anandamide acts as a non-competitive inhibitor on 5-HT_3 receptor-mediated responses in *Xenopus* oocytes. *Synapse* **46:**150–156.
Pacheco MA, Pastoor TE, Lukas RJ, and Wecker L (2001) Characterization of human alpha4beta2 neuronal nicotinic receptors stably expressed in SH-EP1 cells. *Neurochem Res* **26:**683–693.
Pacher P, Batkai S, and Kunos G (2006) The endocannabinoid system as an emerging target of pharmacotherapy. *Pharmacol Rev* **58:**389–462.
Paradiso KG and Steinbach JH (2003) Nicotine is highly effective at producing desensitization of rat alpha4beta2 neuronal nicotinic receptors. *J Physiol* **553:**857–871.
Poling JS, Rogawski MA, Salem N, and Vicini S (1996) Anandamide, an endogenous cannabinoid inhibits Shaker-related voltage-gated K^+ channels. *Neuropharmacology* **35:**983–991.
Quick MW and Lester RA (2002) Desensitization of neuronal nicotinic receptors. *J Neurobiol* **53:**457–478.
Sher E, Chen Y, Sharples TJ, Broad LM, Benedetti G, Zwart R, McPhie GI, Pearson KH, Baldwinson T, and De Filippi G (2004) Physiological roles of neuronal nicotinic receptor subtypes: new insights on the nicotinic modulation of neurotransmitter release, synaptic transmission and plasticity. *Curr Top Med Chem* **4:**283–297.
Spivak CE, Oz M, Beglan CL, and Shrager RI (2006) Diffusion delays and unstirred layer effects at monolayer cultures of Chinese hamster ovary cells: radioligand binding, confocal microscopy, and mathematical simulations. *Cell Biochem Biophys* **45:**43–58.
Tapper AR, McKinney SL, Nashmi R, Schwarz J, Deshpande P, Labarca C, Whiteaker P, Marks MJ, Collins AC, and Lester HA (2004) Nicotine activation of alpha4* receptors: sufficient for reward, tolerance, and sensitization. *Science* **306:**1029–1032.
Viveros MP, Marco EM, and File SE (2006) Nicotine and cannabinoids: parallels, contrasts and interactions. *Neurosci Biobehav Rev* **30:**1161–1181.
Wu J, Kuo YP, George AA, Xu L, Hu J, and Lukas RJ (2004) beta-Amyloid directly inhibits human $\alpha4\beta2$-nicotinic acetylcholine receptors heterologously expressed in human SH-EP1 cells. *J Biol Chem* **279:**37842–37851.

Address correspondence to: Dr. Charles Spivak, National Institute on Drug Abuse, Intramural Research Program, Cellular Neurobiology Branch, Electrophysiology Unit, 5500 Nathan Shock Drive, Baltimore, MD 21224. E-mail: cspivak@intra.nida.nih.gov